

LETTER TO THE EDITOR

The astrophysical parameters of chemically peculiar stars from automatic methods

E. Paunzen¹

Department of Theoretical Physics and Astrophysics, Masaryk University, Kotlářská 2, 611 37 Brno, Czech Republic
e-mail: epaunzen@physics.muni.cz

ABSTRACT

Context. The chemically peculiar (CP) stars of the upper main sequence are excellent astrophysical laboratories for investigating the diffusion, mass loss, rotational mixing, and pulsation in the presence and absence of a stable local magnetic field. For this, we need a homogeneous set of parameters, such as effective temperature (T_{eff}) and surface gravity ($\log g$), to locate the stars in the Hertzsprung-Russell diagram so that we can then estimate the mass, radius, and age.

Aims. In recent years, the results of several automatic pipelines have been published; these use various techniques and data sets, including T_{eff} and $\log g$ values for millions of stars. Because CP stars are known to have flux anomalies, these astrophysical parameters must be tested for their reliability and usefulness. If the outcome is positive, these can be used to analyse the new and faint CP stars published recently.

Methods. I compared published T_{eff} and $\log g$ values of a set of CP stars, which are mostly based on high-resolution spectroscopy, with values from four automatic pipeline approaches. In doing so, I searched for possible correlations and offsets.

Results. I present a detailed statistical analysis of a comparison between the ‘standard’ and published T_{eff} and $\log g$ values. The accuracy depends on the presence of a magnetic field and the spectral type of the CP subgroups. However, I obtain standard deviations of between 2% and 20%.

Conclusions. Considering the statistical errors, the astrophysical parameters from the literature can be used for CP stars, although caution is advised for magnetic CP stars.

Key words. stars: chemically peculiar – stars: fundamental parameters – Hertzsprung-Russell and C-M diagrams

1. Introduction

The chemically peculiar (CP) stars of the upper main sequence have been targets of astrophysical study since their discovery by the American astronomer Antonia Maury (1897). Most of the early research was devoted to detecting peculiar features in their spectra and to characterising their photometric behaviour.

According to Preston (1974), CP stars are commonly subdivided into four classes: metallic line (or Am) stars (CP1), magnetic Ap stars (CP2), HgMn stars (CP3), and He-weak stars (CP4). The CP1 stars are A- and early F-type objects and are defined by the discrepancies found in the spectral types derived from the strengths of the Ca II K line and the hydrogen and metallic lines. In comparison to the spectral types derived from the hydrogen lines, the Ca II K-line types appear too early, and the metallic-line types too late. CP1 stars do not show strong, global magnetic fields (Aurière et al. 2010) and are characterised by underabundances of calcium and scandium and overabundances of the iron peak and heavier elements. CP1 stars are primarily members of binary systems with orbital periods in the range between 2 and 10 days, and their rotational velocities are believed to have been reduced by tidal interactions, which has enabled diffusion to act (Abt 2009). The observed abundance pattern of CP1 stars is defined by the diffusion of elements and the disappearance of the outer convection zone associated with helium ionisation because of the gravitational settling of helium (Théado et al. 2005). These latter authors predict a cut-off rotational velocity for such objects (about 100 km s^{-1}), above

which meridional circulation leads to a mixing in the stellar atmosphere.

The CP2 stars are distinguished by their strong, globally organised magnetic fields that range up to several tens of kG (Bychkov et al. 2021a). In CP2 (and CP4) stars, due to additional magnetic diffusion, the chemical abundance concentrations at the magnetic poles, as well as the spectral and related photometric variabilities, are also easily understood, as are the radial velocity variations of the appearing and receding patches on the stellar surface (Alecian 2015). These inhomogeneities are responsible for the strictly periodic changes observed in the spectra and brightness of many CP2 stars, which are explained by the oblique rotator model (Stibbs 1950). Therefore, the observed periodicity of variation is the rotational period of the star.

The CP3 stars are characterised by strong lines of ionised Hg and/or Mn with overabundances by up to six orders of magnitude relative to their solar abundances (Ghazaryan et al. 2018). Several mechanisms play significant roles in our understanding of these extreme peculiarities: radiatively driven diffusion, mass loss, mixing, light-induced drift, and possibly weak magnetic fields. However, no satisfactory model exists to explain the abundance pattern (Adelman et al. 2003).

The CP4 stars are the hottest CP objects up to early B-types, where the mass-loss and stellar winds become significant (Cidale et al. 2007). Initially, the CP4 stars were defined as He-weak stars only. Later on, it was proposed that this class also includes He-strong stars (Pedersen & Thomsen 1977). However, the latter are rare and are not included in the present analysis. The He lines

Table 1. Coefficients of the corrections ΔT_{eff} and $\Delta \log g$ of the four investigated references. The meaning is $T_{\text{eff}}^{\text{corr}} = a + T_{\text{eff}}^{\text{publ}} + (bT_{\text{eff}}^{\text{publ}})$ and $\log g^{\text{corr}} = a + \log g^{\text{publ}} + (b \log g^{\text{publ}})$. The values by Stassun et al. (2019) could not be checked for the $\log g$ of CP4 stars because they include an insufficient number of objects. If no values a and b are listed, the published astrophysical parameters can be used as they are. The quantity σ gives the standard deviation of the calibrated parameter from the ‘standard value’ from Ghazaryan et al. (2018, 2019) in per cent. The errors in the final digits of the corresponding quantity are given in parentheses.

| | ΔT_{eff} | | | $\Delta \log g$ | | | N |
|--|-------------------------|-------------|-----------------|-----------------|-------------|-----------------|-----|
| | a | b | σ (%) | a | b | σ (%) | |
| Anders et al. (2019, 2022) | | | | | | | |
| CP1 | +896(616) | -0.123(77) | 3.6 | +1.46(50) | -0.377(126) | 4.3 | 54 |
| CP2 | | | 12.7 | | | 8.9 | 83 |
| CP3 | +8554(1276) | -0.664(114) | 8.8 | 2.45(54) | -0.623(136) | 4.9 | 49 |
| CP4 | | | 17.4 | | | 10.8 | 8 |
| Stassun et al. (2019) | | | | | | | |
| CP1 | | | 2.2 | +1.53(25) | -0.387(63) | 3.8 | 102 |
| CP2 | +1698(496) | -0.157(48) | 9.2 | +3.77(61) | -0.953(156) | 8.9 | 125 |
| CP3 | +7986(725) | -0.617(62) | 8.6 | +2.50(68) | -0.633(173) | 4.8 | 86 |
| CP4 | +10377(1426) | -0.695(90) | 10.8 | | | | 10 |
| Fouesneau et al. (2023) | | | | | | | |
| CP1 ($T_{\text{eff}}^{\text{publ}} < 8500$ K) | | | 2.2 | +2.30(43) | -0.569(110) | 4.5 | 58 |
| CP2 | | | 11.7 | +3.32(79) | -0.832(202) | 15.5 | 71 |
| CP3 | +5491(1154) | -0.411(97) | 8.3 | +3.00(35) | -0.764(92) | 6.2 | 65 |
| CP4 | +2707 | | 12.5 | | | 8.6 | 9 |
| Zhang et al. (2023) | | | | | | | |
| CP1 | +4283(288) | -0.552(35) | 4.5 | +2.79(15) | -0.705(39) | 4.1 | 74 |
| CP2 | +5613(237) | -0.659(17) | 7.7 | +3.19(16) | -0.773(46) | 8.8 | 93 |
| CP3 | +10592(619) | -0.891(36) | 9.9 | +3.41(14) | -0.842(42) | 5.4 | 63 |
| CP4 | +11990(2531) | -0.768(132) | 8.2 | +3.69(16) | -0.899(52) | 4.6 | 13 |

of these objects are anomalously weak or strong for their spectral type (effective temperature). The shape of the Balmer continuum of CP4 stars differs from that predicted by models with standard solar helium abundances. Also, these stars display H α emission (especially He-strong stars) and spectroscopic and photometric variability (North 1984), as well as variations in line intensities, radial velocities, luminosity, colour, and magnetic field strength (Pedersen & Thomsen 1977).

Many new and relatively faint CP stars have been discovered (Qin et al. 2019; Hümmerich et al. 2020; Paunzen et al. 2021; Shang et al. 2022) thanks to the new spectroscopic data from the *Gaia* satellite (Andrae et al. 2023) and the Large Sky Area Multi-Object Fibre Spectroscopic Telescope (Cui et al. 2012, LAMOST). For further statistical analysis, we need the astrophysical parameters of our target stars (T_{eff} , $\log g$ or luminosity, and mass). In order to be able to draw robust conclusions, it is most important that we obtain homogeneity in these parameters. Netopil et al. (2008) showed that due to the abnormal colours, determining T_{eff} for CP stars using photometry is not straightforward. These authors presented a comprehensive study of the three main photometric systems (Johnson, Geneva, and Strömgren-Crawford) together with a new relation for bolometric correction. However, such photometric data are unavailable for the newly discovered CP stars.

A way out of this dilemma is to use astrophysical parameters automatically determined by pipeline software based on various photometric and spectroscopic data. This Letter presents a statistical analysis comparing the T_{eff} and $\log g$ from high-resolution spectroscopy and four automatic methods. I searched for offsets and calculated corrections in order to improve the published astrophysical parameters for all subgroups of CP stars.

2. Target selection and used calibrations

The CP stars published by Ghazaryan et al. (2018, 2019) were taken to test the astrophysical parameters. These authors compiled well-established objects with abundances deduced from high-resolution spectroscopic observations. Therefore, most of the T_{eff} and $\log g$ values are also based on these spectra, making them independent of any photometric calibrations. For further analysis, 96 CP1, 133 CP2, 87 CP3, and 18 CP4 stars were extracted. The following approaches were used to determine the astrophysical parameters of the target stars, and the corresponding lists were matched using either coordinates or *Gaia* identifications.

Anders et al. (2019, 2022, StarHorse2021): These authors combined parallaxes and photometry from the *Gaia* DR3 together with the photometric catalogues of Pan-STARRS 1 (Magnier et al. 2013), 2MASS (Skrutskie et al. 2006), ALLWISE (Cutri & et al. 2013), and the SkyMapper DR2 Onken et al. (without the u filter; 2019) to derive Bayesian stellar parameters, distances, and extinctions using the StarHorse code (Queiroz et al. 2018). This latter is a Bayesian parameter-estimation code that compares many observed quantities to stellar evolutionary models. Given the set of observations, plus several priors, it finds the posterior probability over a grid of stellar models, distances, and extinctions. *Anders et al. (2019, 2022)* concluded that the systematic errors of the astrophysical parameters are smaller than the nominal uncertainties for most objects.

Stassun et al. (2019, The Revised TESS Input Catalog): The procedure used by these authors is based on the apparent magnitude in the *TESS* bandpass (T), taking into account the stellar evolutionary phases. They used PHOENIX model atmospheres together with photometric data and calibrations from the *Gaia*

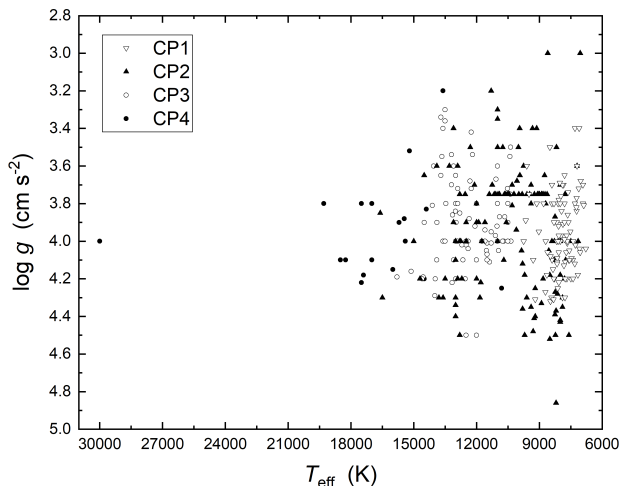


Fig. 1. Hertzsprung-Russell diagram of the target sample. The members of the four CP subgroups are taken from Ghazaryan et al. (2018, 2019).

DR2 and 2MASS catalogues. All calibrations are listed in Stassun et al. (2018).

Fouesneau et al. (2023, Gaia DR3 Apsis): This is the pipeline software developed by the *Gaia* consortium. These authors analysed astrometry, photometry, BP/RP, and RVS spectra for objects across the Hertzsprung-Russell diagram (HRD). Their method was compared and validated with star cluster data, asteroseismological results, and several other references.

Zhang et al. (2023): These authors used *Gaia* DR3 XP spectra to derive astrophysical parameters (T_{eff} , $\log g$, and $[\text{Fe}/\text{H}]$) together with extinction values and corrected parallaxes. They applied a machine-learning model to directly predict stellar parameters from XP spectra with a training set from a model of stellar atmospheric parameters from the LAMOST survey. This approach is superior because it models all relevant parameters significantly affecting the observed spectra. To this end, the authors used 2MASS and WISE photometry.

3. Results and conclusions

I calculated the differences (‘standard’ minus literature value; ΔT_{eff} and $\Delta \log g$) for each CP subgroup and reference for T_{eff} and $\log g$, respectively. I then searched for correlations using these differences. Table 1 presents the results of this statistical analysis.

As can be seen from the last column, the number of available data points varies because the subgroups have different sizes, but also because the hotter stars (CP3 and CP4) are, in general, more difficult to calibrate and are often missing in the automatic analysis. The astrophysical parameters for the CP1 and CP4 stars by Fouesneau et al. (2023) are limited in T_{eff} as listed in Table 1. The $\log g$ values of CP4 stars listed in Stassun et al. (2019) cannot be checked because an insufficient amount of data is available for this class of objects.

No correlations were found between ΔT_{eff} and $\log g$ and between $\Delta \log g$ and T_{eff} . For some combinations, the published values can be used as they are; for example, the values for CP2 stars by Stassun et al. (2019). As a quality indicator, I calculated the quantity σ , which gives the standard deviation of the calibrated parameter from the ‘standard value’ from Ghazaryan

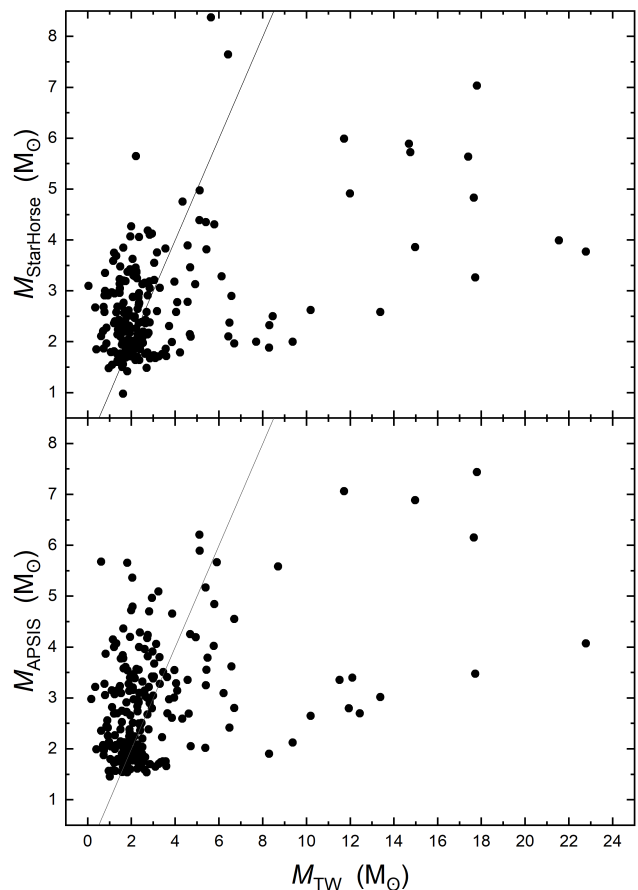


Fig. 2. Comparison of the masses calibrated using the ‘standard’ values from Ghazaryan et al. (2018, 2019) and the ones published by Anders et al. (2022, upper panel) and Fouesneau et al. (2023, lower panel). No clear correlation is visible, and there are many outliers. The sample was not divided into the four subgroups. The abbreviation ‘TW’ means ‘this work’.

et al. (2018, 2019) in per cent. In general, σ is the smallest for the CP1 and CP3 subgroups, which are non-magnetic.

I calculated the mean σ of the individual calibrated T_{eff} and $\log g$ values for all available data, which includes the entire sample of 334 stars, obtaining the following σ values for the four subgroups (CP1-4): [3.3,4.5], [9.5,8.1], [8.6,5.7], and [12.4,7.3].

I then compared the published masses from Anders et al. (2022) and Fouesneau et al. (2023) with those estimated from the ‘standard’ values by Ghazaryan et al. (2018, 2019). The latter publication does not include them, and so I estimated the masses using the luminosity and the formula

$$\log(M/M_{\odot}) = \log(g/g_{\odot}) - 4 \log(T_{\text{eff}}/T_{\text{eff}\odot}) + \log(L/L_{\odot}), \quad (1)$$

with the recommended IAU values for the Sun ($\log g_{\odot} = 4.438$ and $T_{\text{eff}\odot} = 5772$ K). To calculate the individual masses, I used the extinctions from (Paunzen et al. 2024) and Green et al. (2019). The distances were taken from Bailer-Jones et al. (2021) who used the *Gaia* EDR3 and a prior constructed from a three-dimensional model of our Galaxy. Because most of the stars are closer than 500 pc, the reddening can be mostly neglected. The V magnitudes were taken from Kharchenko (2001) and Paunzen (2022). Finally, the bolometric corrections are those from Ne-

Table 2. Ten CP2 stars with exceptionally high masses for their T_{eff} and $\log g$ values. Further investigation is necessary to find the reasons for these apparent anomalies.

| Name | T_{eff} (K) | $\log g$ (cm s^{-2}) | D (pc) | A_V (mag) | M_V (mag) | B.C. (mag) | $\log(L/L_{\odot})$ | M (M_{\odot}) |
|-----------|-------------------------|------------------------------------|-------------|----------------|----------------|---------------|---------------------|------------------------|
| HD 42075 | 7590 | 4.50 | 277 | 0.03 | 1.75 | 0.00 | 1.20 | 6.12 |
| HD 42605 | 8250 | 4.39 | 281 | 0.34 | 1.37 | 0.03 | 1.34 | 4.71 |
| HD 43901 | 8000 | 4.18 | 347 | 0.16 | 0.36 | 0.03 | 1.74 | 8.30 |
| HD 52847 | 8200 | 4.86 | 287 | 0.02 | 0.86 | 0.03 | 1.55 | 22.77 |
| HD 55540 | 8230 | 4.50 | 518 | 0.09 | 0.75 | 0.03 | 1.59 | 10.78 |
| HD 62244 | 8550 | 4.05 | 409 | 0.03 | 0.22 | 0.02 | 1.81 | 5.43 |
| HD 91087 | 8500 | 4.52 | 394 | 0.25 | 1.27 | 0.02 | 1.38 | 6.21 |
| HD 97394 | 8000 | 4.43 | 379 | 0.04 | 0.86 | 0.03 | 1.55 | 9.37 |
| HD 102333 | 8240 | 4.27 | 467 | 0.17 | 0.54 | 0.03 | 1.67 | 7.70 |
| HD 110274 | 8135 | 4.28 | 365 | 0.41 | 1.16 | 0.03 | 1.42 | 4.68 |

topil et al. (2008) for the magnetic CP stars and from Balona (1994) for the non-magnetic CP1 and CP3 objects.

Figure 2 shows the comparison of the different values, from which several conclusions can be made:

- The masses for the CP1 stars generally agree relatively well. These are the coolest and therefore the least massive objects, and are those for which the pipelines are optimised.
- The high-mass end (CP3 and CP4 stars) is underestimated in the literature. Most objects are not included because they are too hot for the pipelines used.
- For ten CP2 stars (listed in Table 2), we find excessively high masses for their T_{eff} and $\log g$ values. This is caused by the high luminosities, for which we have no explanation. No correlations with the known magnetic field strengths (Bychkov et al. 2021b) were found. The reddening values and bolometric corrections are not exceptional. Also, direct conversion of the parallaxes does not change the results. Binarity could play a role, which, for a mass ratio of one, would shift the location by $\Delta M_V = 0.75$ mag, but this is not sufficient to explain the observed high luminosities. From the astrometric measurements by *Gaia*, only three stars (HD 55540, HD 102333, and HD 110274) show hints of being binary systems (Kervella et al. 2019). Additional data, such as classification resolution spectra and a new homogeneous analysis, are needed to shed more light on the nature of these objects and the possible sources of error. However, we can also speculate that the discrepancies found can be used to detect new magnetic CP stars.

I used the correlations presented in the paper by Kılıçoğlu (2021) to verify the masses further. These authors derived a mass–effective-temperature–surface gravity relation for main sequence stars in the range of $6400 < T_{\text{eff}} < 20000\text{K}$ with $\log g > 3.44$, respectively. These ranges cover most of the CP star sample. I checked the results from this calibration in comparison with those from Anders et al. (2022) and Foesneau et al. (2023) for our sample. No correlation exists up to $2.5M_{\odot}$. For larger masses, the values from the literature show some linear relation but are systematically too small.

The presented analysis shows that the published astrophysical parameters, especially for the non-magnetic and cooler CP stars, are statistically functional. With this in mind, several tasks are awaiting future research projects. Many new, faint CP stars have been discovered in recent years for which only masses and ages have been published by Hümmerich et al. (2020). However, the precise location of the objects in the HRD is needed

to fit isochrones. Future studies on the rotational behaviour of CP stars (Faltová et al. 2021) will also require a well-established HRD so that statistically sound conclusions can be drawn.

Acknowledgements. This work was supported by the grant GAČR 23-07605S. I thank Klaus Bernhard, Stefan Hümmerich, and Martin Netopil for discussing various topics and helping to improve the paper significantly. This work has made use of data from the European Space Agency (ESA) mission *Gaia* (<https://www.cosmos.esa.int/gaia>), processed by the *Gaia* Data Processing and Analysis Consortium (DPAC, <https://www.cosmos.esa.int/web/gaia/dpac/consortium>). Funding for the DPAC has been provided by national institutions, in particular, the institutions participating in the *Gaia* Multilateral Agreement. This research has made use of the SIMBAD database, operated at CDS, Strasbourg, France.

References

- Abt, H. A. 2009, *AJ*, 138, 28
Adelman, S. J., Adelman, A. S., & Pintado, O. I. 2003, *A&A*, 397, 267
Alecian, G. 2015, *MNRAS*, 454, 3143
Anders, F., Khalatyan, A., Chiappini, C., et al. 2019, *A&A*, 628, A94
Anders, F., Khalatyan, A., Queiroz, A. B. A., et al. 2022, *A&A*, 658, A91
Andrae, R., Foesneau, M., Sordo, R., et al. 2023, *A&A*, 674, A27
Aurière, M., Wade, G. A., Lignières, F., et al. 2010, *A&A*, 523, A40
Bailer-Jones, C. A. L., Rybizki, J., Foesneau, M., Demleitner, M., & Andrae, R. 2021, *AJ*, 161, 147
Balona, L. A. 1994, *MNRAS*, 268, 119
Bychkov, V. D., Bychkova, L. V., & Madej, J. 2021a, *A&A*, 652, A31
Bychkov, V. D., Bychkova, L. V., & Madej, J. 2021b, *Astronomical and Astrophysical Transactions*, 32, 137
Cidale, L. S., Arias, M. L., Torres, A. F., et al. 2007, *A&A*, 468, 263
Cui, X.-Q., Zhao, Y.-H., Chu, Y.-Q., et al. 2012, *Research in Astronomy and Astrophysics*, 12, 1197
Cutri, R. M. & et al. 2013, *VizieR Online Data Catalog*, II/328
Faltová, N., Kallová, K., Prišegen, M., et al. 2021, *A&A*, 656, A125
Foesneau, M., Frémat, Y., Andrae, R., et al. 2023, *A&A*, 674, A28
Ghazaryan, S., Alecian, G., & Hakobyan, A. A. 2018, *MNRAS*, 480, 2953
Ghazaryan, S., Alecian, G., & Hakobyan, A. A. 2019, *MNRAS*, 487, 5922
Green, G. M., Schlafly, E., Zucker, C., Speagle, J. S., & Finkbeiner, D. 2019, *ApJ*, 887, 93
Hümmerich, S., Paurzen, E., & Bernhard, K. 2020, *A&A*, 640, A40
Kervella, P., Arenou, F., Mignard, F., & Thévenin, F. 2019, *A&A*, 623, A72
Kharchenko, N. V. 2001, *Kinematika i Fizika Nebesnykh Tel*, 17, 409
Kılıçoğlu, T. 2021, *A&A*, 655, A91
Magnier, E. A., Schlafly, E., Finkbeiner, D., et al. 2013, *ApJS*, 205, 20
Netopil, M., Paurzen, E., Maitzen, H. M., North, P., & Hubrig, S. 2008, *A&A*, 491, 545
North, P. 1984, *A&AS*, 55, 259
Onken, C. A., Wolf, C., Bessell, M. S., et al. 2019, *PASA*, 36, e033
Paurzen, E. 2022, *A&A*, 661, A89
Paurzen, E., Hümmerich, S., & Bernhard, K. 2021, *A&A*, 645, A34
Paurzen, E., Netopil, M., Faltová, N., & Prišegen, M. 2024, *A&A*, submitted
Pedersen, H. & Thomsen, B. 1977, *A&AS*, 30, 11
Preston, G. W. 1974, *ARA&A*, 12, 257
Qin, L., Luo, A. L., Hou, W., et al. 2019, *ApJS*, 242, 13
Queiroz, A. B. A., Anders, F., Santiago, B. X., et al. 2018, *MNRAS*, 476, 2556
Shang, L.-H., Luo, A. L., Wang, L., et al. 2022, *ApJS*, 259, 63
Skrutskie, M. F., Cutri, R. M., Stiening, R., et al. 2006, *AJ*, 131, 1163
Stassun, K. G., Oelkers, R. J., Paegert, M., et al. 2019, *AJ*, 158, 138
Stassun, K. G., Oelkers, R. J., Pepper, J., et al. 2018, *AJ*, 156, 102
Stibbs, D. W. N. 1950, *MNRAS*, 110, 395
Théado, S., Vauclair, S., & Cunha, M. S. 2005, *A&A*, 443, 627
Zhang, X., Green, G. M., & Rix, H.-W. 2023, *MNRAS*, 524, 1855